# Performance Assessment of a Cavity on Source ChargePlasmaTFET-Based Biosensor

Mahalaxmi Patil, Anju Gedam, *Student Member, IEEE*, and Guru Prasad Mishra, *Member, IEEE*

***Abstract*—The promising candidate for designing a highly sensitive biosensor is the tunneling field effect transistor (TFET). In this work, for the first time the performance analysis of a cavity on source charge plasma tunneling field effect transistor (CS-CPTFET) based lable-free biosensor has been proposed. To design the device,charge plasma concept is adapted, where suitable metal workfunctions have been used to create the source and drain regions. The charge plasma technique reduces random dopant fluctuation, thermal budget and steps required for the fabrication. The significant advantage of the proposed device includes the creation of abrupt doping profile at the tunneling junction (source-channel).The achievement of abrupt doping profile at the tunneling junction is responsible for the enhanced sensitivity and suppression of negative conduction (ambipolar) since the cavity is created in the source oxide region of CS-CPTFET biosensor. The response of the proposed biosensor for various biomolecules has been analyzed in terms of band energy variation, electric field, surface potential and transfer characteristics by using Silvaco ATLAS device simulator. Various biomolecules such as uricase (k = 1.54), Glucose oxidase (k = 3.46), APTES (k = 3.57), bacteriophage T7 (k = 6.3), keratin (k = 8) and gelatin (k=12) have been considered for examining the performance of proposed biosensor.**

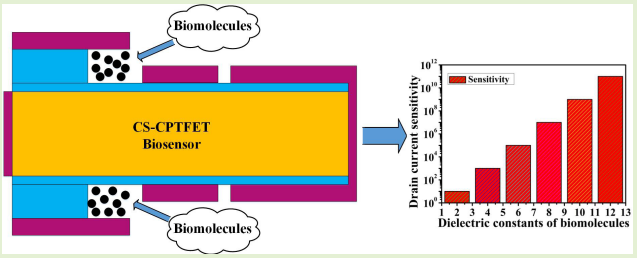


***Index Terms*—Ambipolar, biomolecules, biosensor, charge plasma, sensitivity.**

## I. Introduction

EARLY stage identification and proper diagnosis of the diseases in all lives are challenging on the provision of medical field. The label detection methods such as electrochemical, fluorescent, and magnetic methods change the inherent properties of biomolecules. These methods give inaccurate results and are also time consuming [1]–[3]. So, label-free electrical detection methods, which yield more accurate results, have become the interesting topic of the research [4]. Field effect transistor (FET) based biosensors are compatible for the label-free electrical detection of the biomolecules [5]. The application of biosensor includes food industry, environmental monitoring system, medical industry and so on [6]–[8]. Speed of detection and sensitivity are very important while designing a biosensor [9], [10]. Small size, low cost and capacity of mass production are the beneficial features of FET based biosensors [11]. First FET based biosensor reported by Bergveld in 1970 is ion sensitive field effect transistor (ISFET), which is proficient to detect charged biomolecules, but incompatible to sense the neutral biomolecules, since the target analyte (biomolecule) is present between electrolyte and electrode [12]. The FET based biosensors, which can sense both neutral and charged biomolecules are dielectrically modulated FETs (DMFETs) such as silicon nanowire FET, FinFET, MOSFET and impact ionization FET [13]–[16].The electrical characteristics of DMFETs vary as properties (i.e., dielectric constant (k) and charge density ($N_f$) of biomolecules are changed [17]. So, the efficient coupling between gate and channel forms the working principle of DMFETs. To fulfil the demands of advanced technology, down scaling of the device dimensions is necessary. Down scaled device requires less volume of analyte to detect. After certain limits, miniaturization of MOSFET's dimensions leads to unavoidable problems such as SCEs, high power consumption, and degraded $I_{ON}/I_{OFF}$ ratio. The device, which works on band-to-band tunneling mechanism, resolves these problems is tunneling field effect transistor (TFET) and has been initiated for biosensing applications [18]–[22]. Significant features possessed by TFET are steeper SS (<60mV/decade), the lowest OFF state current and power consumption, faster response, and higher sensitivity [21], [22]. Even though TFET acts as the most efficient substitute of MOSFET, it suffers from unavoidable issues

Manuscript received August 7, 2020; revised September 16, 2020; accepted September 16, 2020. Date of publication September 28, 2020; date of current version January 6, 2021. The associate editor coordinating the review of this article and approving it for publication was Dr. Irene Taurino. *(Corresponding author: Guru Prasad Mishra.)*

The authors are with the Electronics and Communication Engineering Department, National Institute of Technology Raipur, Raipur 492010, India (e-mail: gpscmishra.etc@nitrr.ac.in).

Digital Object Identifier 10.1109/JSEN.2020.3027031

like ambipolar conduction (i.e., negative conduction), poor ON state current [23], [24]. Various mechanisms are adapted to improve ON state current such as introduction of lower bandgap material in the source region, metal workfunction engineering of the electrodes, multi-gate, hetero dielectric materials etc. [25]–[31]. Negative conduction can be overcome by introducing higher bandgap material in the drain region, metal workfunction engineering etc. [32], [33]. Carrier concentration in the channel region can be improved by increasing the source doping concentration compared to doping of drain. This improvement in the electron tunneling rate results in the enhanced ON state current [34], [35]. Achievement of sharp doping profile at source-channel and drain-channel junctions is very difficult, because of random dopant fluctuations (RDFs). Hence, physical doping suffers from fabrication complexity and expensiveness [36], [37]. These shortcomings of conventional TFET can be overcome by charge plasma doping-less technique. Ease of fabrication can be accomplished by charge plasma technique in which adequate metals have been used to build source and drain regions [37]–[39].

This work presents a label-free cavity on source charge plasma TFET based biosensor. As the name suggests, the cavity is formed on source region near the tunneling junction to overcome the solid solubility and to improve the carrier concentration in the channel region. The proposed device can sense both charged and neutral biomolecules in an efficient way. The immobilization of biomolecules in the nanogap cavities changes oxide capacitance, which gets reflected in the electrical characteristics. For examining the device performance various dielectric values of biomolecules are considered. Various biomolecules are used for examining electric field, band energy, transfer characteristics and subthreshold swing of the proposed device [30]–[44]. The ability of the proposed device has been examined through Silvaco ALTAS device simulator [45].

## II. Structural Definition of the Device

The transversal section of CS-CPTFET based label free biosensor is as indicated in Fig. 1. Intrinsic doping concentration ($10^{15}$ $cm^{-3}$) has been considered over the entire device. The nanogaps are incised into the source dielectric material as shown in the design. The doping of drain and source regions in the fabrication has been avoided by the application of Hafnium (3.9 eV) and Platinum (5.93 eV) metals, respectively. Selection of these metals is based on the concept of charge plasma, i.e. the metal for drain can be selected only when $\varphi_D < \chi_{S_i} + E_g/2$ and for source metal it should satisfy $\varphi_S > \chi_{S_i} + E_g/2$. Here, $\chi_{S_i}$ and $E_g$ represent electron affinity (4.17 eV) and bandgap (1.1 eV) of silicon. The thickness ($t_{Si}$) of silicon body considered here is of 10nm, which obeys the Debye's length for smooth operation, above which quantum effects can be ignored [37-38]. The length of source ($L_S$) and drain ($L_D$) regions is 100nm and the channel length ($L_C$) considered is of 50nm. The cavities, in which biomolecules can be placed, hold the length ($L_{Cavity}$) and thickness ($t_{Cavity}$) of 25nm and 5.5nm respectively as shown in Fig .1. Metal workfunction of gate is 4.5 eV. Dielectric

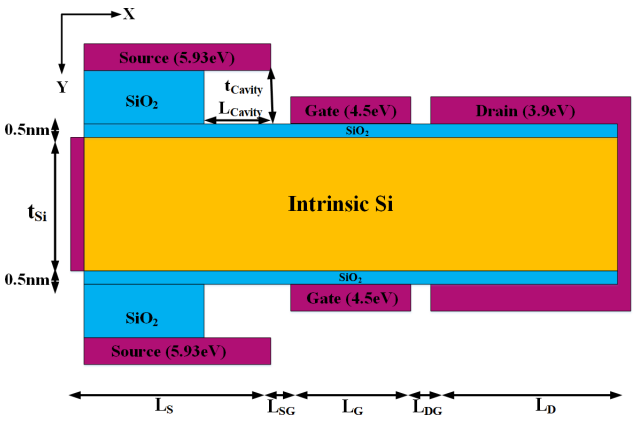


Fig. 1. Transversal view of CS-CPTFET biosensor.

TABLE I
VARIOUS BIOMOLECULES WITH DIELECTRIC CONSTANTS

| Biomolecules | Dielectric constant [30, 41-44] |
|---|---|
| Uricase | 1.54 |
| Biotin | 2.63 |
| 3-aminopropyltriethoxysilane (APTES) | 3.57 |
| Bacteriophage T7 | 6.3 |
| Keratin | 8 |
| Gelatin | 12 |

material $SiO_2$ has been employed as an adhesive material for the biomolecules in the nanogaps and its thickness is 0.5nm. This sacrificial layer helps to get the predicted sensitivity values by suppressing the gate leakage current [25]. The source and drain regions are induced in the proposed device by employing the gaps of 2nm and 5nm between source-gate ($L_{SG}$) and drain-gate ($L_{DG}$) respectively.

During the fabrication of CS-CPTFET based label-free biosensor, the cavities into the source dielectric can be carved by dry etching. Very thin 0.5nm adhesive layer $SiO_2$ can be developed by dry oxidation, which also avoids the silicide formation. The source, gate and drain electrodes can be developed by low pressure chemical vapor deposition (LPCVD) [46], [51]. Biomolecules carry either only dielectric constant (k) or charge density plus dielectric constant ($k+N_f$), based on which they are named as neutral or charged biomolecules. Various biomolecules whose dielectric values are universally accepted have been considered for the validation of the proposed biosensor.

Examination of the proposed device includes the biomolecules such as uricase (used as protein drug to suppress infections on human body caused by uric acid), biotin (belongs to vitamin B family, helps in growth of hair), 3-aminopropyltriethoxysilane (APTES, used for silanization), Bacteriophage T7 (kills many useful bacteria), Keratin and Gelatin (proteins found in nails, skin and hair) [30], [41]–[44]. The corresponding dielectric constant values of these biomolecules are given in table I. Most of the biomolecules have thickness and length less than 2nm and 5nm, respectively. So, they can fit into the nanogap of height 5.5 nm [43], [47]. The combined benefits of doping-less and junction-less TFET are utilized to design the highly sensitive biosensor.

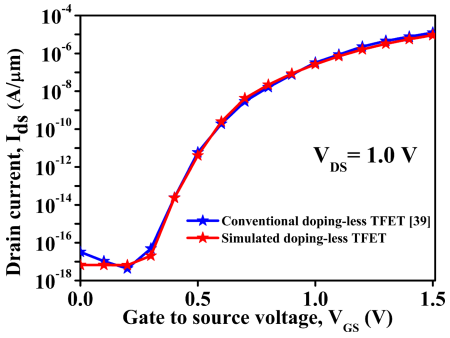


Fig. 2. Evaluation with conventional doping-less TFET [39].

## III. Device Modeling and Calibration

Silvaco ATLAS 2D device simulator is used to carry out the simulation of CS-CPTFET. The tunneling rate calculation at tunneling junction (source-channel) is enabled by considering the nonlocal band-to-band tunneling model. Along with BTBT model, defining of quantum tunneling region at source-channel interface (i.e., tunneling junction) enables tunneling of carriers. The meshing of quantum tunneling region should be dense compared to remaining part of the device for achieving precise sensitivity values. Concentration and field dependent mobilities can be captured by using Lombardi mobility model. Recombination of minority carriers can be enabled by Shockley–Read–Hall and Auger models. Bandgap narrowing and Fermi–Dirac statistics are also included during simulation. Numerical tunneling probability can be activated by Wentzel–Kramers–Brillouin method.

Simulator validation has been demonstrated by considering the same dimensions, models, and parameters of conventional doping-less TFET reported by Kumar and Janardhanan [39]. The simulated transfer characteristics at $V_{DS} = 1V$ is in good agreement with conventional result, which validates the simulator is shown in Fig. 2.

## IV. Results and Discussion

The response of CS-CPTFET biosensor for both neutral and charged biomolecules is discussed in this section. The effects of various biomolecules (mentioned in table I) on the device performance have been measured by replacing air ($k = 1$) in the nanogap cavities under source electrode with dielectric values ($k > 1$) and charge density ($N_f = \pm 10^{10}$ to $10^{12}$ C cm$^{-2}$). Maximum tunneling barrier width can be seen when cavities are empty ($k = 1$) compared to the presence of neutral biomolecules. The reason behind this is the introduction of neutral biomolecules in the cavities increases the capacitance under the source electrode. So, the coupling between source electrode and source region increases. The charge density of biomolecules is considered at the interface of Si-$SiO_2$ along with entire cavity region. The reference value throughout the analysis has been considered at $k = 1$.

In this section, the results are discussed in terms of carrier density, surface potential, band energies, transfer characteristics, $I_{ON}/I_{OFF}$ ratios and SS. Under OFF ($V_{GS} = 0$ V, $V_{DS} = +1.0$ V) and ON ($V_{GS} = +1.5$ V, $V_{DS} = +1.0$ V) state, the carrier concentration in source, channel and drain regions of the device are shown in Fig. 3. It can be seen that,

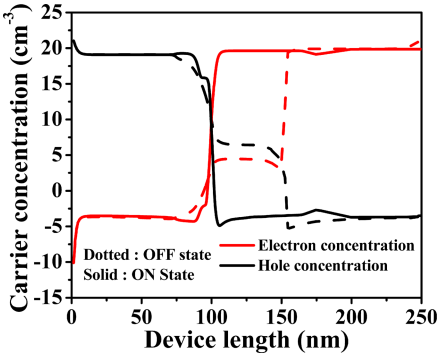


Fig. 3. Electron and hole concentrations of CS-TFET biosensor in OFF and ON states.

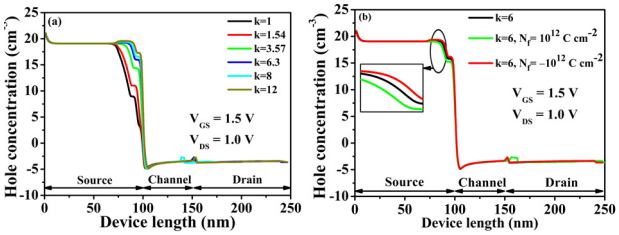


Fig. 4. Hole concentration variation in source region due to (a) neutral (b) charged biomolecules.

by using charge plasma concept, hole carrier concentration of $\sim 10^{20}$cm$^{-3}$ can be induced in the source region and electron carrier concentration of $\sim 10^{20}$ cm$^{-3}$ in the drain region under both OFF and ON states. The concentration of electrons in the channel is high under the ON state due to the application of gate bias and it results in higher tunneling rate.

Variation of hole concentration in the source region as a function of dielectric constant values of neutral biomolecules is presented in Fig. 4(a). It can be percieved that, the capacitive coupling between source region and its electrode increases with an increament in the dielectric constant of biomolecules. Due to this, the concentarion of hole under the cavity increases leading to the abrupt junction (abrupt doping profile) between source and the channel. Fig. 4(b) defines the variation of hole concentration in the source region due to charged biomolecules. When negative chareged biomolecules are trapped into the cavities, these attract more number of holes into the source region leading to steepness at the tunneling junction (source-channel). The contradict behavior can be observed in case of positive charged biomolecules (decrement of hole concentration in source region).

The reflection of presence of biomolecules on the band energy along the device length under the OFF and ON state is depicted in Fig. 5(a). This plot depicts that, there is no band alignment (i.e., between valence band (VB) of source and conduction band (CB) of the channel) even though biomolecules are fully filled in the cavities under OFF state represented by dotted lines. The application of gate bias increases the gate control over the channel and it reduces the tunneling barrier as shown by solid lines. Now, as the dielectric constant increases the tunneling barrier width decreases further. This is because of the enhancement in the hole concentration in source, which results in maximum tunneling rate. In Fig. 5(b),

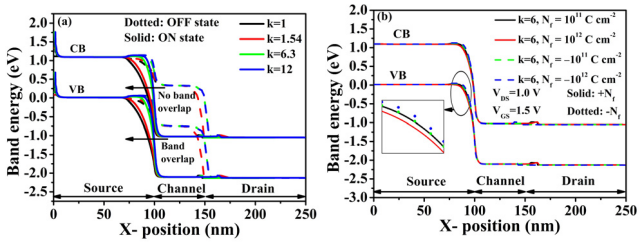


Fig. 5. Band energy variation of CS-CPTFET due to (a) neutral, (b) charged biomolecules.

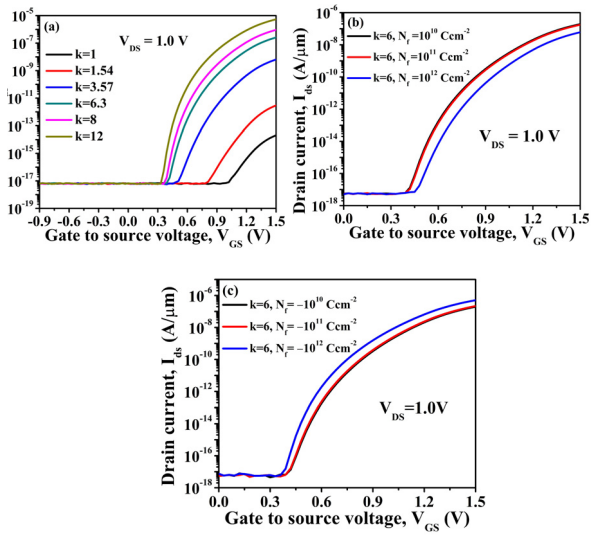


Fig. 6. Transfer characteristics of CS-CPTFET due to (a) Neutral, (b) Positive, (c) Negative charged biomolecules.

the solid lines show the widening of tunneling barrier when positive charge density of the biomolecules is increased. Since, the positive charge in the cavity attracts the electrons leading to the decrement of holes in the source region. So, the control between source electrode and the source region decreases due to the positive charged biomolecules in the cavities. The abrupt doping profile between source-channel can be achieved with an increment of negative charge density of biomolecules. So, compaction in the tunneling barrier can be observed in case of negatively charged biomolecules as shown by the dotted lines.

With an increase in dielectric constant value of biomolecules in the nanogap cavities, the density of holes in the source region increases. This induced layer of holes under the cavity in the source region increases the alignment between the VB of source and CB of channel. This decreased tunneling barrier is responsible for enhanced tunneling of electrons. Hence, the increased tunneling rate causes increment in ON current.Fig. 6(a) depicts the impact of neutral biomolecules on the transfer characteristics. It can also be noticed that, the ambipolar conduction is suppressed in the proposed model. The peak current achieved by the proposed model is $5.5 \times 10^{-6}$ A/$\mu$m at k = 12. Enhancement of the positive charge density in the cavities decreases the concentration of holes in the source region. This leads to increment in the barrier at source-channel junction. Hence, there is decrement in the drain current ($I_{ds}$), which is described by Fig. 6(b). The presence of

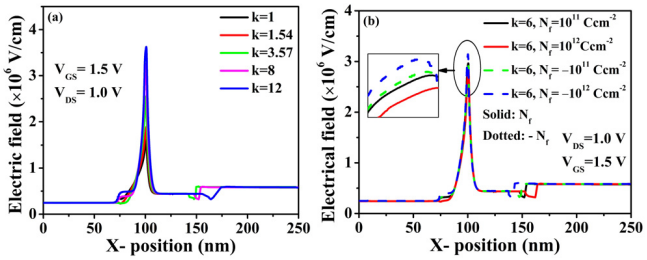


Fig. 7. Electric field of CS-CPTFET along the device length for (a) neutral, (b) charged biomolecules.

negative charged biomolecules in the cavities attracts a greater number of holes. This improvement in the source impurity concentration enables the decrement in the tunneling barrier and improves the tunneling rate. So, the ON current elevates with an increment in the negative charge density as portrayed in Fig. 6(c).

The generation of sharp doping profile with an increment in the dielectric values of immobilized biomolecules in the cavities causes the improvement of electric field at tunneling junction. The plot of variation in the electric field of CS- CPTFET for the neutral biomolecules is shown in Fig. 7(a). An electric field of $1.64 \times 10^6$V/cm can be reached at the tunneling junction for k = 12. The reflection of positive charge density variation (from $N_f = 10^{10}$ C cm$^{-2}$ to $10^{12}$ C cm$^{-2}$) on the electric field is depicted in Fig. 7(b) by solid lines. The electric field decreases for an increment in the positive charge density due to the expansion in the width of tunneling barrier. The elevation in the electric field is observed when negative charge density is increased and is denoted by dotted lines.

The sensitivity quantifies a proficient biosensor, which is essential for its design. So, the sensitivity of any biosensor should be as high as possible which symbolizes, how efficiently it detects the target biomolecule. The sensitivity of CS-CPTFET biosensor is computed in respect of drain current for both charged and neutral biomolecules and is given by [30]

$$S_{I_{ds}} = \left( \frac{I_{ds}^{bio} - I_{ds}^{air}}{I_{ds}^{air}} \right) \tag{1}$$

In equation (1), empty cavities give the drain current represented by $I_{ds}^{air}$ and completely filled cavity yield the drain current mentioned as $I_{ds}^{bio}$. So, the sensitivity values of various biomolecules have been calculated by using CS-CPTFET biosensor.The higher dielectric (k > 1) values of biomolecules result in higher drain current ($I_{ds}$) and higher drain current results in higher sensitivity. The reflection of neutral and charged biomolecules on sensitivity values is mentioned in table II. It can be noted from table II that, the sensitivity values decrease with an increment in the positive charge density of biomolecules due to the decrement in the tunneling rate. The $I_{ds}$ value increases with an elevation in the negative charge density and shows the increased sensitivity. The highest sensitivity of the proposed biosensor is obtained at moderate $V_{GS}$, because of rapid increment of $I_{ds}$ in subthreshold region of TFET.

Impact of both charged and neutral biomolecules on $I_{ON}/I_{OFF}$ ratio is illustrated in Fig. 8 (a-b). Improvement

TABLE II
SENSITIVITY VALUES OF CS-CPTFET BIOSENSOR DUE TO NEUTRAL, POSITIVE AND NEGATIVE CHARGED BIOMOLECULES

| Employed Biomolecules | Dielectric constant values(k) | Sensitivity ($V_{GS}$ = 1.5 V and $V_{DS}$=1.0 V) |
|---|---|---|
| Neutral Biomolecules | 1.54 | $2.54\times10^{2}$ |
| | 3.57 | $3.71\times10^{6}$ |
| | 6.3 | $3.83\times10^{8}$ |
| | 8 | $1.87\times10^{9}$ |
| | 12 | $1.73\times10^{10}$ |
| Positive Charged ($+N_f$) Biomolecules | k=6, $N_f$= $10^{10}$ C/cm$^2$ | $2.67\times10^{8}$ |
| | k=6, $N_f$= $10^{11}$ C/cm$^2$ | $2.32\times10^{8}$ |
| | k=6, $N_f$= $10^{12}$ C/cm$^2$ | $1.34\times10^{7}$ |
| Negative Charged ($-N_f$) Biomolecules | k=6, $N_f$= $-10^{10}$ C/cm$^2$ | $2.75\times10^{8}$ |
| | k=6, $N_f$= $-10^{11}$ C/cm$^2$ | $3.15\times10^{8}$ |
| | k=6, $N_f$= $-10^{12}$ C/cm$^2$ | $1.07\times10^{9}$ |

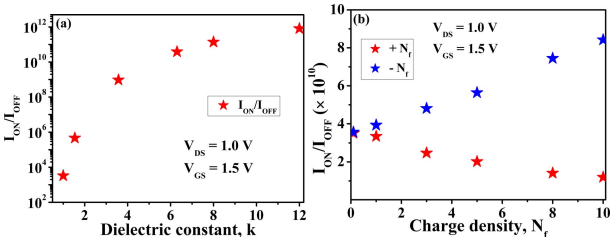


Fig. 8. $I_{ON}/I_{OFF}$ ratio of CS-CPTFET biosensor for (a) neutral, (b) charged biomolecules.

in the dielectric constant forms the sharp doping profile at source-channel junction. Increment in the hole concentration in source region reduces barrier width i.e., the alignment between CB of channel and VB of source increases. Because of this, the tunneling of electrons increases. Hence, the ratio of $I_{ON}/I_{OFF}$ increases with dielectric constant as depicted in Fig. 8(a). Influence of charged biomolecules on $I_{ON}/I_{OFF}$ ratio is shown in Fig. 8(b), where X- axis represents the magnitude of charge density of biomolecules. The positive charge density in the cavities increases tunneling width. So, reduction in the ON current results in the degradation of $I_{ON}/I_{OFF}$ ratio. Attraction of hole by negative charge in the cavities improves the ON current and $I_{ON}/I_{OFF}$ ratio.

The voltage ($V_{GS}$), which causes one-decade increment in the drain current ($I_{ds}$) of a device is characterized as subthreshold swing (SS). SS value is essential for categorizing a biosensor as an efficient biosensor i.e., lower is the SS faster is the device performance. The SS of TFET based biosensor is given by [39], which is represented as below:

$$SS = \left(\frac{\Delta V_{GS}}{\Delta \log(I_{ds})}\right) \text{mV/decade} \tag{2}$$

Unlike FET (based on thermionic emission), SS of TFET (tunneling phenomenon) is a function of gate to source voltage ($V_{GS}$) as indicated in equation (2). The performance of CS-CPTFET biosensor can also be evaluated by SS. Fig. 9(a-b) shows the variation of SS as a function of dielectric constant (k) and charge density ($\pm$ $N_f$) of various biomolecules. The accumulation of higher dielectric biomolecule induces

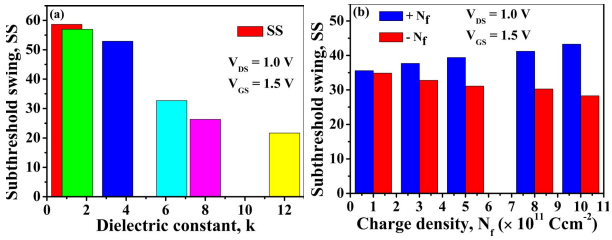


Fig. 9. Influence of (a) neutral, (b) charged biomolecules on SS.

TABLE III
COMPARISON OF SENSITIVITY VALUES

| | Sensitivity value | Reference |
|---|---|---|
| Dielectric constant of biomolecule (k=12) | $2.59\times10^{7}$ | [46] |
| | $5.45\times10^{9}$ | [48] |
| | $4.75\times10^{5}$ | [49] |
| | $1.04\times10^{6}$ | [50] |
| | $1.73\times10^{10}$ | Proposed |

the sharper junction between channel and source. Thinner tunneling junction enables higher tunneling rate. So, SS of the proposed device shows the reduction with an elevation in dielectric constant (k = 1, 1.54, 3.57, 6.3, 8 and 12), which is plotted in Fig. 9(a) and it illustrates the superior performance of the proposed device. In the same manner, the SS increases (decreases) for positive (negative) charged biomolecules, because of widening (thinning) of barrier at the junction, which is depicted in Fig. 9(b) and the magnitude of charge density is taken along X- axis of the figure.

The sensitivity value obtained by proposed model at k = 12 is compared with the previous works [46], [48]–[50] are mentioned in table III. The sensitivity values of the reported works are extracted by using web plot digitizer.

The proposed biosensor is capable of detecting single biomolecule immobilized in the cavities and this specifies the limit of detection. To ensure this, single molecule of Urate oxidase (Uricase) having thickness 1.2 nm and length 5nm in the cavities has been considered [47]. The sensitivity value of 0.255 is obtained for single uricase molecule in the cavities.

## V. CONCLUSION

This work presents a new model of TFET based biosensor for a label free electrical detection. Proficient detection of various (both neutral and charged) biomolecules has been done by CS-CPTFET label-free biosensor. Exploitation of cavities under source electrode by etching out the source dielectric, results in the sharp doping profile at the tunneling junction of the device. The concept of charge plasma and cavity into source dielectric enable the reduction of fabrication complexity and steeper edge at source-channel junction. The electrical parameters such as band energy, transfer characteristics, electric field, $I_{ON}/I_{OFF}$ and SS have been studied under the application of neutral and charged biomolecules. During the simulation, the steeper subthreshold swing (SS) achieved by this model is 21.7 mV/decade. Peak drain current ($I_{ds}$) of $5.5\times10^{-6}$ A/$\mu$m and an electric field of $1.64\times10^{6}$ V/cm are

obtained at k = 12. The highest $I_{ON}/I_{OFF}$ ratio obtained by this model is $8.09 \times 10^{11}$. The most important parameter to declare the proposed model as a potential biosensor is sensitivity; the maximum sensitivity achieved is $1.73 \times 10^{10}$. By analyzing all the electrical parameters and its immunity to RDFs, this model can be used as a proficient biosensor for detecting the biomolecules.

## REFERENCES


[1] G. Marrazza *et al.*, "Disposable DNA electrochemical sensor for hybridization detection," *Biosensors Bioelectron.*, vol. 14, no. 1, pp. 43–51, Jan. 1999.

[2] M. Bras, J.-P. Cloarec, F. Bessueille, E. Souteyrand, J.-R. Martin, and J.-P. Chauvet, "Control of Immobilization and hybridization on DNA chips by fluorescence spectroscopy," *J. Fluorescence*, vol. 10, no. 3, pp. 247–253, Feb. 2000.

[3] M. M. Miller *et al.*, "A DNA array sensor utilizing magnetic microbeads and magnetoelectronic detection," *J. Magn. Magn. Mater.*, vol. 225, nos. 1–2, pp. 138–144, Jan. 2001.

[4] D.-Y. Jang, "Sublithographic vertical gold nanogap for label-free electrical detection of protein-ligand binding," *J. Vac. Sci. Technol. B, Microelectron.*, vol. 25, no. 2, pp. 443–447, Apr. 2007.

[5] D. Abdi and M. J. Kumar, "Dielectric modulated overlapping gate-on-drain tunnel-FET as a label-free biosensor," *Superlattices Microstruct.*, vol. 86, pp. 98–202, Oct. 2015.

[6] B. J. Schaertel and R. Firstenbergeden, "Biosensors in the food industry: Present and future," *J. Food Protection*, vol. 51, no. 10, pp. 811–820, Oct. 1988.

[7] V.-T. Nguyen, Y. S. Kwon, and M. B. Gu, "Aptamer-based environmental biosensors for small molecule contaminants," *Current Opinion Biotechnol.*, vol. 45, pp. 15–23, Jun. 2017.

[8] B. D. Malhotra, S. Kumar, and C. M. Pandey, "Nanomaterials based biosensors for cancer biomarker detection," *J. Phys., Conf. Ser.*, vol. 704, pp. 1–11, Apr. 2016.

[9] M. Barbaro, A. Bonfiglio, and L. Raffo, "A charge-modulated FET for detection of biomolecular processes: Conception, modeling, and simulation," *IEEE Trans. Electron Devices*, vol. 53, no. 1, pp. 158–166, Jan. 2006.

[10] C. H. Kim, C. Jung, H. G. Park, and Y.-K. Choi, "Novel dielectric modulated field-effect transistor for label-free DNA detection," *Bio Chip J.*, vol. 2, no. 2, pp. 127–134, 2008.

[11] A. C. Seabaugh and Q. Zhang, "Low-voltage tunnel transistors for beyond CMOS logic," *Proc. IEEE*, vol. 98, no. 12, pp. 2095–2110, Dec. 2010.

[12] P. Bergveld, "Development of an ion-sensitive solid-state device for neurophysiological measurements," *IEEE Trans. Biomed. Eng.*, vol. BME-17, no. 1, pp. 70–71, Jan. 1970.

[13] A. Gao *et al.*, "Enhanced sensing of nucleic acids with silicon nanowire field effect transistor biosensors," *Nano Lett.*, vol. 12, no. 10, pp. 5262–5268, Oct. 2012.

[14] G. A. T. Sevilla, M. T. Ghoneim, H. Fahad, J. P. Rojas, A. M. Hussain, and M. M. Hussain, "Flexible nanoscale high-performance FinFETs," *ACS Nano*, vol. 8, no. 10, pp. 9850–9856, Oct. 2014.

[15] J.-T. Park and J.-P. Colinge, "Multiple-gate SOI MOSFETs: Device design guidelines," *IEEE Trans. Electron Devices*, vol. 49, no. 12, pp. 2222–2229, Dec. 2002.

[16] N. Kannan and M. J. Kumar, "Dielectric-modulated impact-ionization MOS transistor as a label-free biosensor," *IEEE Electron Device Lett.*, vol. 34, no. 12, pp. 1575–1577, Dec. 2013.

[17] J. M. Choi, J. W. Han, S. J. Choi, and Y. K. Choi, "Analytical modelling of a nanogap-embedded FET for application as a biosensor," *IEEE Trans. Electron Devices*, vol. 57, no. 12, pp. 3477–3484, Dec. 2010.

[18] P. Dwivedi and A. Kranti, "Applicability of transconductance-to-current ratio ($gm/I_{ds}$) as a sensing metric for tunnel FET biosensors," *IEEE Sensors J.*, vol. 17, no. 4, pp. 1030–1036, Feb. 2017.

[19] S. Kanungo, S. Chattopadhyay, P. S. Gupta, and H. Rahaman, "Comparative performance analysis of the dielectrically modulated full- gate and short-gate tunnel FET-based biosensors," *IEEE Trans. Electron Devices*, vol. 62, no. 3, pp. 994–1001, Mar. 2015.

[20] R. Narang, M. Saxena, and M. Gupta, "Comparative analysis of dielectric-modulated FET and TFET-based biosensor," *IEEE Trans. Nanotechnol.*, vol. 14, no. 3, pp. 427–435, May 2015.

[21] W. Y. Choi, B.-G. Park, J. Duk Lee, and T.-J. King Liu, "Tunneling field-effect transistors (TFETs) with subthreshold swing (SS) less than 60 mV/dec," *IEEE Electron Device Lett.*, vol. 28, no. 8, pp. 743–745, Aug. 2007.

[22] P. F. Wang *et al.*, "Complementary tunnelling transistor for low power application," *Solid-State Electron.*, vol. 48, no. 12, pp. 2281–2286, 2004.

[23] A. Hraziia, A. Vladimirescu, A. Amara, and C. Anghel, "An analysis on the ambipolar current in Si double-gate tunnel FETs," *Solid-State Electron.*, vol. 70, pp. 67–72, Apr. 2012.

[24] S. Saurabh and M. J. Kumar, "Novel attributes of a dual material gate nanoscale tunnel field-effect transistor," *IEEE Trans. Electron Devices*, vol. 58, no. 2, pp. 404–410, Feb. 2011.

[25] S. Kanungo, S. Chattopadhyay, P. S. Gupta, K. Sinha, and H. Rahaman, "Study and analysis of the effects of SiGe source and pocket-doped channel on sensing performance of dielectrically modulated tunnel FET-based biosensors," *IEEE Trans. Electron Devices*, vol. 63, no. 6, pp. 2589–2596, Jun. 2016.

[26] B. R. Raad *et al.*, "Physics-based simulation study of high-performance gallium arsenide phosphide–indium gallium arsenide tunnel field-effect transistor," *IET Micro Nano Lett.*, vol. 11, no. 7, pp. 366–368, Jul. 2016.

[27] B. R. Raad, K. Nigam, D. Sharma, and P. N. Kondekar, "Performance investigation of bandgap, gate material work function and gate dielectric engineered TFET with device reliability improvement," *Superlattices Microstructures*, vol. 94, pp. 138–146, Jun. 2016.

[28] R. Vishnoi and M. J. Kumar, "Compact analytical drain current model of gate-all-around nanowire tunneling FET," *IEEE Trans. Electron Devices*, vol. 61, no. 7, pp. 2599–2603, Jul. 2014.

[29] G. Dewey *et al.*, "Fabrication, characterization, and physics of III–V heterojunction tunneling field effect transistors (H-TFET) for steep subthreshold swing," in *IEDM Tech. Dig.*, Dec. 2012, vol. 10, no. 1109, pp. 33.6.1–33.6.4.

[30] M. Mahalaxmi, B. Acharya, and G. P. Mishra, "Design and analysis of dual-metal-gate double-cavity charge-plasma-TFET as a label free biosensor," *IEEE Sensors J.*, early access, Mar. 6, 2020, doi: 10.1109/JSEN.2020.2979016.

[31] A. Bhattacharyya, M. Chanda, and D. De, "Performance assessment of new dual-pocket vertical heterostructure tunnel FET-based biosensor considering steric hindrance issue," *IEEE Trans. Electron Devices*, vol. 66, no. 9, pp. 3988–3993, Sep. 2019.

[32] D. B. Abdi and M. Jagadesh Kumar, "Controlling ambipolar current in tunneling FETs using overlapping gate-on-drain," *IEEE J. Electron Devices Soc.*, vol. 2, no. 6, pp. 187–190, Nov. 2014.

[33] K. Nigam, P. Kondekar, and D. Sharma, "Approach for ambipolar behaviour suppression in tunnel FET by workfunction engineering," *Micro Nano Lett.*, vol. 11, no. 8, pp. 460–464, Aug. 2016.

[34] J. Min, J. Wu, and Y. Taur, "Analysis of source doping effect in tunnel FETs with staggered bandgap," *IEEE Electron Device Lett.*, vol. 36, no. 10, pp. 1094–1096, Oct. 2015.

[35] C. Sandow, J. Knoch, C. Urban, Q.-T. Zhao, and S. Mantl, "Impact of electrostatics and doping concentration on the performance of silicon tunnel field-effect transistors," *Solid-State Electron.*, vol. 53, no. 10, pp. 1126–1129, Oct. 2009.

[36] S. Agarwal, G. Klimeck, and M. Luisier, "Leakage-reduction design concepts for low-power vertical tunneling field-effect transistors," *IEEE Electron Device Lett.*, vol. 31, no. 6, pp. 621–623, Jun. 2010.

[37] B. Ghosh and M. W. Akram, "Junctionless tunnel field effect transistor," *IEEE Electron Device Lett.*, vol. 34, no. 5, pp. 584–586, May 2013.

[38] C. Sahu and J. Singh, "Charge-plasma based process variation immune junctionless transistor," *IEEE Electron Device Lett.*, vol. 35, no. 3, pp. 411–413, Mar. 2014.

[39] M. J. Kumar and S. Janardhanan, "Doping-less tunnel field effect transistor: Design and investigation," *IEEE Trans. Electron Devices*, vol. 60, no. 10, pp. 3285–3290, Oct. 2013.

[40] Ajay, R. Narang, M. Saxena, and M. Gupta, "Modeling and simulation investigation of sensitivity of symmetric split gate junctionless FET for biosensing application," *IEEE Sensors J.*, vol. 17, no. 15, pp. 4853–4861, Aug. 2017.

[41] G. Löffler, H. Schreiber, and O. Steinhauser, "Calculation of the dielectric properties of a protein and its solvent: Theory and a case study," *J. Mol. Biol.*, vol. 270, no. 3, pp. 520–534, Jul. 1997.

[42] A. Cuervo, P. D. Dans, J. L. Carrascosa, M. Orozco, G. Gomila, and L. Fumagalli, "Direct measurement of the dielectric polarization properties of DNA," *Proc. Nat. Acad. Sci. USA*, vol. 111, no. 35, pp. E3624–E3630, Aug. 2014.

[43] S. Kim, D. Baek, J.-Y. Kim, S.-J. Choi, M.-L. Seol, and Y.-K. Choi, "A transistor-based biosensor for the extraction of physical properties of from biomolecules," *Appl. Phys. Lett.*, vol. 101, no. 7, Aug. 2012, Art. no. 073703.
[44] A. Paliwal, M. Tomar, and V. Gupta, "Complex dielectric constant of various biomolecules as a function of wavelength using surface plasmon resonance," *J. Appl. Phys.*, vol. 116, no. 2, Jul. 2014, Art. no. 023109.
[45] *ATLAS Device Simulation Software*, Silvaco, Santa Clara, CA, USA, 2016.
[46] R. Goswami and B. Bhowmick, "Comparative analyses of circular gate TFET and heterojunction TFET for dielectric-modulated label-free biosensing," *IEEE Sensors J.*, vol. 19, no. 21, pp. 9600–9609, Nov. 2019.
[47] N. Colloch *et al.*, "Crystal structure of the protein drug urate oxidase-inhibitor complex at 2.05 Å resolution," *Nature Struct. Mol. Biol.*, vol. 4, 514no. 11, pp. 947–952, Nov. 1997.
[48] S. Anand, A. Singh, S. I. Amin, and A. S. Thool, "Design and performance analysis of dielectrically modulated doping-less tunnel FET-based label free biosensor," *IEEE Sensors J.*, vol. 19, no. 12, pp. 4369–4374, Jun. 2019.
[49] G. Wadhwa and B. Raj, "Label free detection of biomolecules using charge-plasma-based gate underlap dielectric modulated junctionless TFET," *J. Electron. Mater.*, vol. 47, no. 8, pp. 4683–4693, Aug. 2018.
[50] V. D. Wangkheirakpam, B. Bhowmick, and P. D. Pukhrambam, "N+ pocket doped vertical TFET based dielectric-modulated biosensor considering non-ideal hybridization issue: A simulation study," *IEEE Trans. Nanotechnol.*, vol. 19, pp. 156–162, 2020.
[51] R. J. E. Hueting, B. Rajasekharan, C. Salm, and J. Schmitz, "The charge plasma P-N diode," *IEEE Electron Device Lett.*, vol. 29, no. 12, pp. 1367–1369, Dec. 2008.

**Mahalaxmi Patil** received the B.E. degree in electronics and communication engineering from the Appa Institute of Engineering and Technology Gulbarga, India, in 2016. She is currently pursuing the M.Tech. degree in VLSI design and embedded systems with the National Institute of Technology Raipur, India.

Her current research interests include TFET and nanoscale devices for biosensing applications.

**Anju Gedam** (Student Member, IEEE) received the B.E. degree in electronics and telecommunication engineering from CSVTU Bhilai, India, in 2013, and the M.Tech. degree in micro-nano electronics from the PDPM Indian Institute of Information Technology, Design and Manufacturing, Jabalpur, India, in 2017. She is currently pursuing the Ph.D. degree in electronics and communication engineering with the National Institute of Technology Raipur, Raipur, India. Her current research interests include tunnel field-effect transistor and its applications, nanoscale device design, and biosensor.

**Guru Prasad Mishra** (Member, IEEE) received the B.E. degree in electronics engineering from Utkal University, the M.Tech. degree from NIT Rourkela, Rourkela, India, and the Ph.D. degree in electron devices from Jadavpur University, Kolkata, India, in 2012. He is working as an Associate Professor at the National Institute of Technology Raipur. His current research interests include design, simulation, micro and nano device.